# VISUALIZING RELATIONS USING THE "OBSERVABLE REPRESENTATION"

L. S. SCHULMAN*,‡ and J. P. BAGROW*,†,§

*Physics Department,
Clarkson University, Potsdam,
New York 13699-5820, USA

†Center for Complex Networks Research
and Department of Physics,
Northeastern University, Boston, MA 02115, USA
‡schulman@clarkson.edu
§bagrowjp@clarkson.edu

B. GAVEAU

Laboratoire analyse et physique mathématique,
14 avenue Félix Faure, 75015 Paris, France
gaveau@ccr.jussieu.fr

The *observable representation* provides an embedding of a discrete space in a low dimensional continuous space. Typically, the discrete space is a model of a complex system. This graphical representation is known to highlight significant properties of the original space and can serendipitously reveal unanticipated relationships. We report on the current status of this technique and give examples of its applications and rationale.

*Keywords*: Embeddings; stochastic processes; observable representation.

## 1. Introduction

The *observable representation* is a way of imaging relationships between objects. Sometimes it gathers together items that are closely related, sometimes it puts them on a line. Occasionally it will link objects that you might not have guessed have any connection. And often the actual distance between points carries useful meaning. The technique has been applied in several ways, but particularly with models of complex systems may be expected to aid in the analysis. Briefly, its power arises because it looks at a transformation of the dynamics (or neighbor-to-neighbor relationships) that gathers far-flung information, much as the Fourier transform does. This remark will be elaborated below.

Mathematically, the observable representation is an embedding of a space, usually discrete, in $\mathbb{R}^n$, for some $n$. In the original formulation [1–3], the space was the

set of states of a Markov process, but then we found that a great deal of useful information was conveyed even without that interpretation [4]. The basic idea is that there is a matrix (of transition probabilities between states for the Markov process) and one looks at the "slowest" eigenvectors of that matrix, usefully interpreted as "observables" (see below for more on this interpretation). Call the underlying space (that you want to embed) $X$ and call the matrix $R$. For $x, y \in X$, let $A_k(x)$ be a left eigenvector of eigenvalue $\lambda_k$, so that $\lambda_k A_k(x) = \sum_y A_k(y) R_{yx}$. Now select a collection of eigenvectors $A_{k_1}(x), A_{k_2}(x), \ldots, A_{k_m}(x)$. Then it is easy to state what the observable representation (OR) is: it is the set of points $\{\boldsymbol{A}(x) \mid x \in X\}$, where the boldface "$\boldsymbol{A}$" represents the vector: $\boldsymbol{A}(x) \equiv (A_{k_1}(x), A_{k_2}(x), \ldots, A_{k_m}(x))$. For visualization, "$m$" is typically 2 or 3, although for other purposes (e.g. identifying points on the convex hull) higher dimensions enter. In this context "slow" means that $\lambda_k$ is near 1, since the maximum (and slowest) eigenvalue of a stochastic matrix is one.

The ease of definition is deceptive. There is a wealth of information built into this set, since each eigenvector responds to the entire matrix, $R$. As remarked, this resembles a kind of multi-dimensional Fourier analysis (and in some examples is exactly that), a dual way of visualizing the space $X$. And, as stated above, since each $\boldsymbol{A} \in \mathbb{R}^m$, it is an embedding of $X$ in Euclidean $m$-space (see Fig. 8 for a discussion of complex eigenvectors).

To see why we call the embedding the "observable representation" we recall the statistical mechanics background of these ideas and in particular why, under appropriate circumstances, the left eigenvectors of $R$ play the role of observables. The context is the study of phase transitions. In [2], we showed that first-order phase transitions are associated with eigenvalue degeneracy near the stationary state (that which has eigenvalue 1). When that happens, the right eigenvectors, when restricted to a phase, are (to a good approximation) proportional to the probability distributions within that phase, while the left eigenvectors are nearly constant on each phase (and are different in different phases). The left eigenvector can thus be thought of as the "name" of the phase; it allows one to say, "this is ice", "this is water", since it characterizes what is common to the entire phase. In [5], we go further. First, as for the conventional use of the word observable, the left eigenvector can be *emergent*. For example, in a particular Ising model and above the transition temperature, the first left eigenvalue is just the magnetization. Furthermore, we found that the left eigenvectors can have similar interpretations when our methods are applied outside the context of phase transitions.

Some of our methods and conclusions are similar to those of "spectral clustering" [6, 7], although the two forms of analysis have arisen from entirely different pursuits. In the observable representation we invariably work with stochastic matrices (reflecting, for example, Monte Carlo approaches to the Ising model), which are sometimes relevant in other applications as well (cf., in Sec. 3, our Markov process interpretation of Zachary's karate club [8]). This context yields a number of theorems helpful in the interpretation of the images, for example, the

use of barycentric coordinates for calculating probabilities and inequalities relating transition probabilities and OR distance (see below). The phase transition background for our work makes natural the clustering interpretation, although the opposite extreme, in which *many* eigenvalues cluster around the slowest, has also yielded surprising information. In particular, it allows a visualization of an underlying space, whether it be Brownian motion on that space or Brownian motion on a power set of that space (cf. [4]). The latter investigations also arose from a phase transition orientation, in particular the desire to include critical phenomena (a.k.a. second order phase transitions) as objects of our technique.

In this article we will show examples where we mostly understand what is going on. That's Sec. 2. Then (Sec. 3) we show several figures, taken from ecology, cell biology and genetics, where useful information does appear, but whose theoretical basis is less well-understood. To be specific, various points (representing constructs of the underlying study, e.g. taxa, proteins, patient tissues) are placed in a suggestive relation to one another, but the practitioner needs to think about what this "suggestion" means! In the first two of these examples we have hints, while in the third there are real indications of — at the least — diagnostic value. Then in Sec. 4 we recall some of what has actually been proved in previous works as well as give new material on the interpretation of the OR; but we emphasize that interpretation is an ongoing project.

## 2. Examples Involving Stochastic Processes

Let $\xi(t)$ be a random walk on a $15 \times 15$ lattice. Let there be a bump in the middle and let the walker prefer[a] to go downhill. The landscape is shown in Fig. 1. Associated with this Markov process there is a matrix of transition probabilities, $R$. For example,

$$R_{(2,3)(2,4)} = \Pr[\xi(t+1) = (2,3) \,|\, \xi(t) = (2,4)] = \textit{Probability that the process is}$$
$$\textit{at the point (2,3) at time-}(t+1), \textit{ given that it was at (2,4) at time } t.$$

The left eigenvectors of $R$ are designated $A_0(x)$, $A_1(x)$, etc., with $A_0$ the function that is 1 on all states. (The fact that $A_0$ has eigenvalue 1 corresponds to conservation of probability for the process; thus $A_0(y) = 1 = \sum_x A_0(x)R_{xy} = \sum_x R_{xy}$: from $y$ you go *somewhere*.) Figure 2 shows the OR for $k = 1, 2, 3$, that is, the set of points $\{(A_1(x), A_2(x), A_3(x)) \,|\, x = (k, \ell), k, \ell = 1, \ldots, 15\}$.

The first thing to notice is that the set is contained within a tetrahedron and that nearly 200 of the 225 points are clustered in the vertices of that figure. Actually, you cannot really notice the clustering, since they are so close together, but an

---

[a] "Prefer" in this context means that we have a Monte Carlo program in which the relative probabities of going uphill or downhill have the ratio $\exp(-\Delta V/T)$, with $V$ the altitude in Fig. 1 and $T$ the effective temperature, chosen low enough for the "mountain" to be a significant impediment.
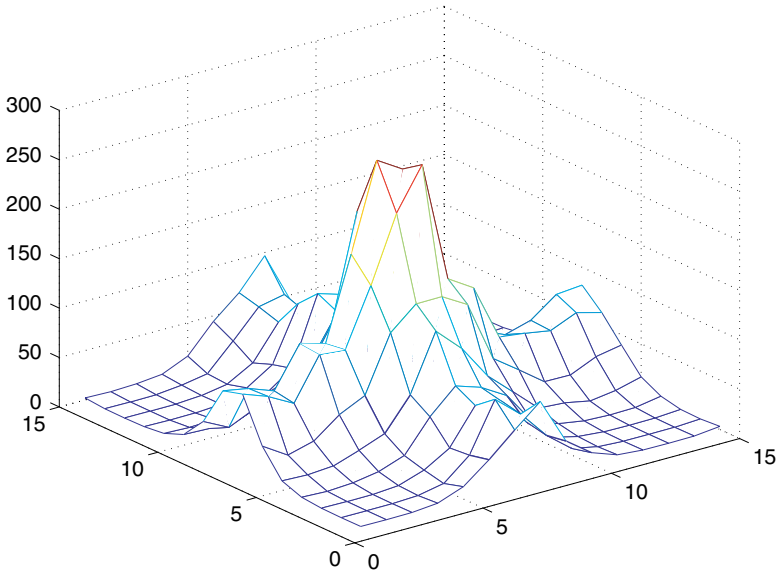
Fig. 1.   (Color online) Landscape for a random walk on a $15 \times 15$ lattice (left). The "walker" wanders from point to (adjacent) point on the lattice, preferring to go downhill, but occasionally climbing. The distance unit on the lattice is arbitrary and the scale of the altitudes chosen so as to give a dynamical spectrum illustrating the OR.
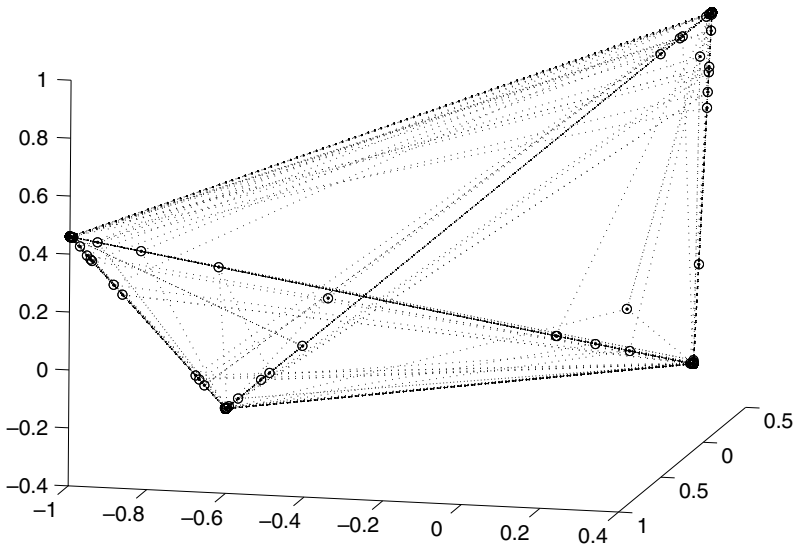


Fig. 2.   Observable representation (OR) for the random walk on the landscape pictured in Fig. 1. Each circle represents a point on the lattice and its position within the tetrahedron (when expressed in barycentric coordinates with respect to the extremals) gives the probability of starting at that point and arriving at one or another extremal. Lines are drawn only to guide the eye: the convex hull of the OR in this case is a tetrahedron.

Fig. 3. Enlargement, by a factor 300 (with some rotation), of the upper right hand vertex of Fig. 2. There are still nearly coincident points at the extremum even with this enlargement.

enlargement, Fig. 3, shows this to be the case (see also [3] for such a blow-up of a vertex of an apparent triangle).

The same computer program that generates the diagram can also label which point is which. That is, if you were to focus on one of the points of the OR you can know which location (i.e. point $(k, \ell) \in X$) it is. (This figure does not have such labeling.) The 4 collections of vertex points correspond to the four basins of attraction of the landscape. Non-vertex points are those that in the long run have a significant probability of ending up in more than one possible basin of attraction. These are points at the top of the "hill" or on the top of the ridges between basins. Further precision can also be achieved: write the OR-location of an intermediate point using the *barycentric* coordinates with respect to the vertices of the tetrahedron (these are the extrema of this OR; see Appendix A for the definition of barycentric coordinates). These coordinates sum to one, and the coefficient (coordinate) with respect to a given extremum is the probability that starting from the point in question the process will, for long times, find itself in the neighborhood of that extremum. Proof of these assertions can be found in [3].

A particular feature of the matrix $R$ for the illustrated random walk is that its spectrum of eigenvalues has, besides the usual "1" (representing conservation of probability and the existence of a stationary state), 3 additional eigenvalues that are quite close to 1. Moreover, there is a gap between these 4 leading (largest in magnitude) eigenvalues and all others. This is characteristic of a multiphase phase
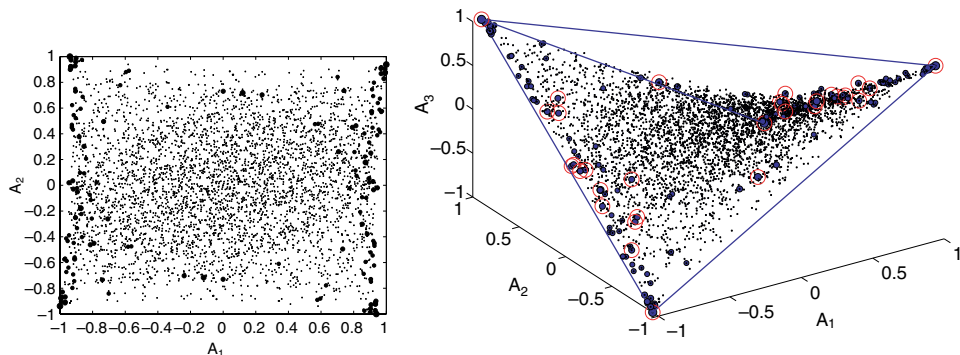
Fig. 4.   (Color online) Observable representation (OR) for a particular quench of a mean field spin glass.

transition. As we will see, when these ideas are applied to graphs, this eigenvalue and eigenvector structure can also characterize graphs in which there are well-defined communities. (This is because on a graph with communities, travel within a community along the graph is more likely than leaving a community.)

Even without the gap, the extrema can indicate phases of varying lifetime (in Markov process terms these would be regions of $X$-space where the system could be caught and spend a lot of time). A system of considerable interest is the *spin glass*, known for its subtle properties as well as for its extremely long relaxation times — something that makes those subtle properties all the more difficult to divine. In Fig. 4 is the OR for the leading non-trivial eigenvalues in the mean field spin glass [10].[b] The $A_1$ versus $A_2$ plot is *not* a simplex because the dimension is too low. Nevertheless, the extrema represent stable or metastable phases. In dimension 3, this looks like a tetrahedron, with the two lines on the left and the right being at right angles to one-another in this embedding. As you continue to increase dimension, more extrema appear, representing shorter-lived metastable states. These assertions were checked by studying both the extremal structure of the convex hull of the OR as well as the energies and dynamical properties (in a stochastic dynamics simulation) of the particular states of the spin glass.

We have also explored the OR when there is neither gap nor near-degeneracy. Many of our theorems do not apply. Nevertheless, the OR recovers information implicit in the transition rate rules — in particular the geometry of an underlying space. As a simple example, consider Brownian motion on a discrete circle. By this we mean that the particle can randomly move from $k$ ($1 \leq k \leq N$) to $k \pm 1$, with

[b]The figure was generated for the Sherrington–Kirkpatrick model [9] which has $N$ $\pm 1$-valued spins, $\sigma_k$, and an interaction energy $E = -\sum J_{k\ell}\sigma_k\sigma_\ell/\sqrt{N}$, where $J_{k\ell}$ is a collection of quenched interaction coefficients. They too take the values $\pm 1$.
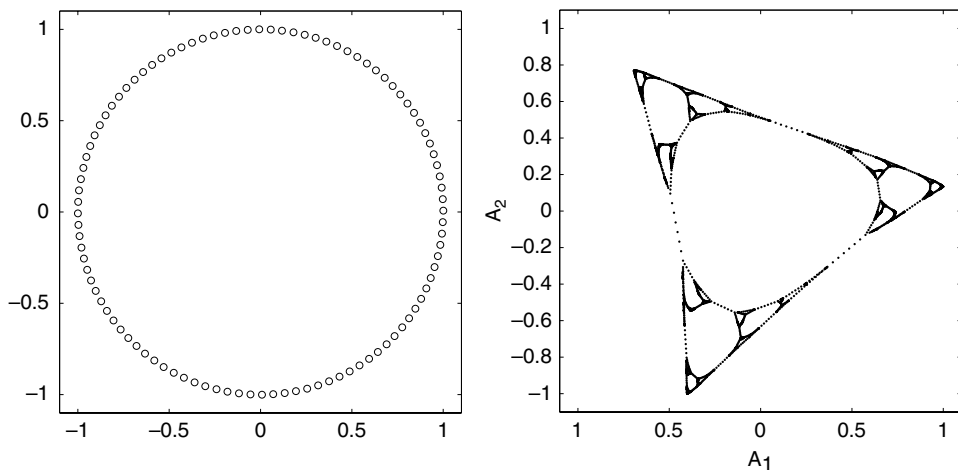
Fig. 5.   ORs for Brownian motion on a circle and on a fractal. Magnification of the latter reveals further fractal structure; see Ref. 4 for a detail of this figure, as well as a graph of the eigenfunctions.

modulo-$N$ addition (so 0 is the same point as $N$). The OR for this motion is shown in Fig. 5. More dramatic is the OR for a random walk on a fractal, Fig. 5. (*Note*: This figure is *not* a picture of the space). It is the OR (from computing the eigenvectors for the walk on the fractal) — and the OR reproduces the space! A case of particular interest is the OR for low-temperature Kawasaki (spin-conserving) stochastic dynamics on a one-dimensional Ising model with periodic boundary conditions. Remarkably, this reveals the geometry of the *underlying* space — not the space of spins — which in this case is basically a circle. This demonstrates that built into the OR is also the ability to detect properties of spatial correlations, an important correlate of 2nd order phase transitions. See Ref. 4, where many other examples are given.

## 3.  Examples Involving Graphs

A famous graph is that associated with Zachary's karate club [8]. This club, comprised of 34 individuals, was the subject of an anthropological study in which individuals were considered either connected or not, based on Zachary's assessment of their relationship; hence the graph. Subsequently the club split and that graph was studied (by us and by many others [12]) to see if it predicted the composition of the split components.

A graph is abstractly given by an adjacency matrix and one can think of this as a stochastic process. Perhaps for a karate club a Frisbee game would be insufficiently dynamic, but one could imagine that if they *did* play Frisbee, they would toss it to those to whom they are connected according to Zachary's study. The Markov process is then the succession of Frisbee tossers. With this interpretation, if $A$ is

the adjacency matrix (all 0's and 1's), then $R_{k\ell} = A_{k\ell}/\sum_j A_{j\ell}$.[c] The reason we sum over $j$ in the denominator is that $R_{k\ell}$ is the probability that $\ell$ tosses to $k$. This implies that the sum over $k$ must be 1, since $\ell$ tosses it to *somebody*. For other graphs, the relation between $A$ and $R$ can be different, and other interpretations are possible.

With this prescription, our study of the karate club [14] gave more or less the breakup that actually occurred. Our criteria were based on the OR, although without the visualization that we now find so useful. In this, we followed earlier work on coarse graining in statistical mechanics [5]. (Again we refer to our articles for details.)

We next collect graphs of biological interest. The OR message in these is not always clear; nevertheless, it *is* clear that there is a message.

Our first example is from ecology, a trophic food web, or biomass transfer network, of the Florida Everglades and associated regions [15–17]. We then discuss a protein interaction network for yeast [18, 19]. Finally we deal with an epigenetic pseudo-dynamics, specifically, a matrix in which distances are a function of the closeness of tissue samples based on gene expression. Tantalizing results show that the OR provides useful information in all these settings. For the last case, in particular, there is a strong indication that the OR could have predictive or diagnostic value.

### 3.1. *A trophic food web*

A trophic food web tracks how biomass, represented by carbon, moves through a system of organisms within a particular ecosystem. The network is composed of a number of *compartments*, representing individual species, groups of related species, or other entities such as the collection of organic particulates.[d] The amounts of biomass exchanged between pairs of compartments, in kilograms of carbon per square meter, then defines the network.

To create an OR we define a pseudo-dynamics. For this example, we define the transition matrix $R$ (between compartments) to be proportional to the biomass transfers. Specifically, $R_{ij} = T_{ij}/\sum_k T_{kj}$, where $T_{ij}$ is the amount of biomass transferred from compartment-$j$ to compartment-$i$. In other words, a unit of carbon moves through the system with transfer probabilities proportional to the amounts

---

[c]The ambiguity in going from an arbitrary $N \times N$ irreducible matrix with non-negative elements to a stochastic matrix is characterized by an $N$-vector, call it $f(x)$, $x \in X$. For suppose you had a stochastic matrix, $R$. Replace each off-diagonal element, $R_{xy}$, by $R_{xy}/f(y)$ and adjust the diagonal term so that the column sum is unity. (The condition $0 \le R_{xy} \le 1$ restricts the class of $f$'s.) The new matrix is obviously stochastic and if $p_0(x)$ was the stationary state of the original matrix, $p_0(x)f(x)$ is the new stationary state. Note though that currents are unaffected by this transformation. This transformation can, however, seriously affect the OR. Nevertheless, in our experience, choosing any of a variety of simple methods for making a matrix stochastic did not affect our qualitative results.

[d]Note that the same authors use the word "compartments" in other senses as well [11].

of biomass being exchanged. An important detail, however, is that these food webs are not closed systems; they have both input and output, and there is an exchange of material with the ambient environment. Omitting such transfers would lead to an apparent non-conservation of biomass. To overcome this, we add a connection from the output compartments to an input, ensuring conservation. This effectively creates reservoirs (as in systems in contact with heat baths at different temperatures) and allows currents in the stationary state.

We focus on a comprehensive study of the food web in Florida Bay [16], a tropical lagoon in the Florida Keys and a series of mangrove-lined bays at the southern end of the Florida peninsula. Our data are taken from the material on the researchers' website, http://www.cbl.umces.edu/~atlss/FBay001.html.

In Fig. 6, we show a plot of the connections between compartments, using conventional graphing techniques. Due to the dense number of connections between compartments, this graph is not informative.

By contrast, the OR, Fig. 7, is more manageable. It (automatically) groups the compartments into related categories (primary producers, fishes, etc.). The lines connect points on the faces of the convex hull. The most evident feature is that the primary producers and detritus define the outer limits of the convex hull and are
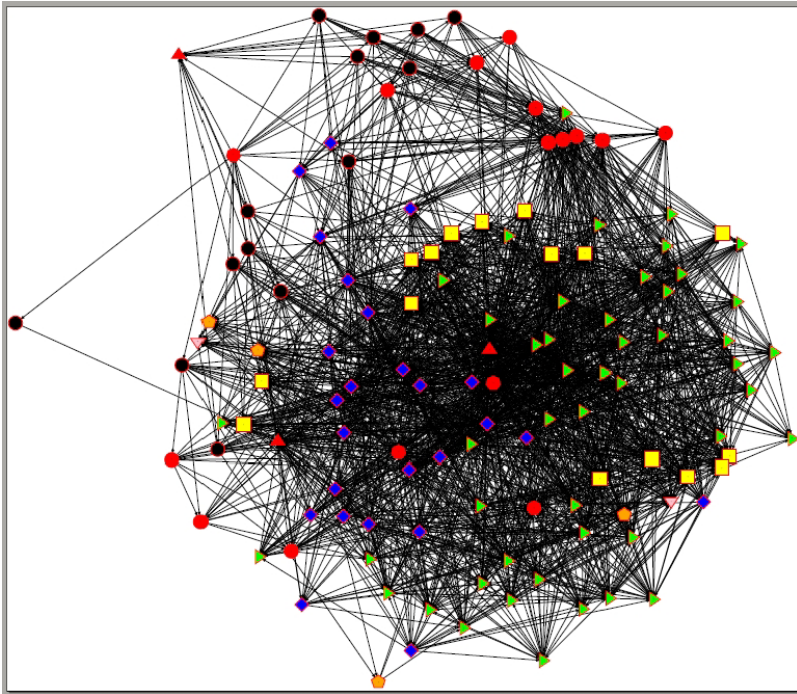


Fig. 6. (Color online) The Florida Bay trophic network in which node locations are determined by the Graphviz force-spring algorithm [13]. Symbols roughly correspond to the categories used in Figs. 6 and 8.
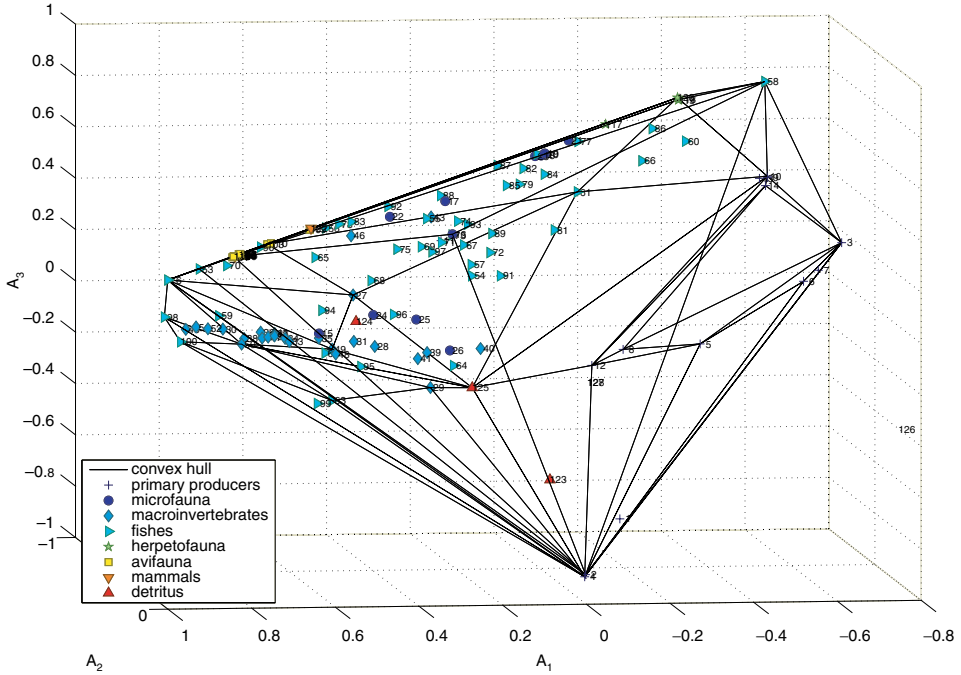
Fig. 7.   (Color online) OR for the first 3 eigenvectors of the Florida Bay C transfer graph. Each point represents a compartment, and symbols indicate similar compartment types. The numbers correspond to the listing in [16].

largely outside the plane occupied by most of the other categories. A conceptually similar sorting takes place in a collection of keywords drawn from the literature of complexity theory [20]. The keywords of greatest generality gravitate to the outside, while those that are more specific are in the interior.

   We next collect a number of observations based on this graph and others. In the present article we do not provide all the evidence for these observations: not only would the number of figures required be prohibitive, but much of our information is best gleaned by real-time rotations of the figures, using the same software as was employed for generating the graphs (MATLAB®). In addition we would some-times enlarge symbols for some taxa or categories of taxa, to allow more holistic comprehension of the data.

   Note that some points cluster, but not in the fashion observed in the phase transition ORs (see Figs. 2 and 4). This occurs because (as we checked in detail) the clustered taxa are nourished to a large extent by the same source (or for the transpose matrix, are either eaten by or decay to the same compartment). The theory behind this goes back to the definition of the vectors in the OR, to wit:

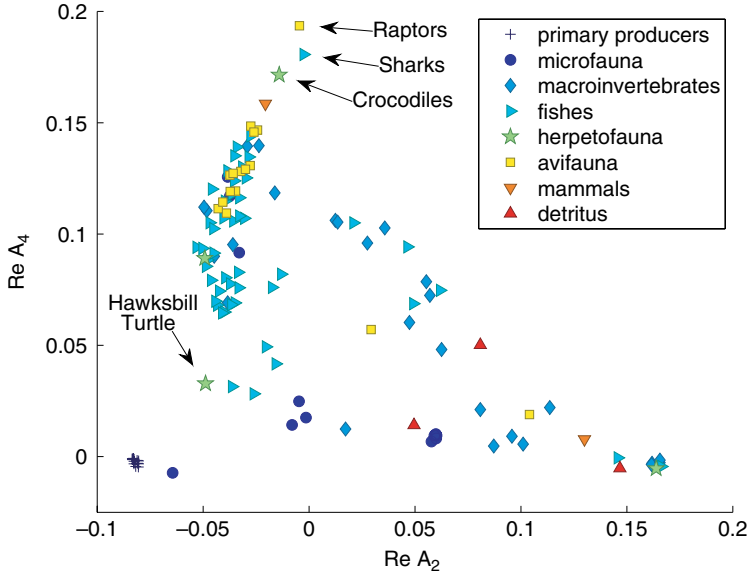$$\lambda_k A_k(x_0) = \sum_y A_k(y) R_{yx_0}. \tag{1}$$

Fig. 8. (Color online) The OR of the Florida Bay biomass transfer network. As above, each point represents a compartment. Several interesting compartments have been annotated, showing the "top of the food chain" animals as well as the critically endangered Hawksbill Turtle. Note that points have been slightly displaced for clarity (without this some points lie atop one another, as in the vertices of Fig. 2). This figure, plotting real and imaginary parts of eigenvectors, also illustrates another point. For many applications, $R$ can have complex eigenvalues and eigenvectors. But because $R$ itself is real, both eigenvalues and eigenvectors come in complex conjugate pairs. In this case it can be useful to plot real and imaginary parts of the eigenvectors.

Suppose that several taxa, $x_1, x_2, x_3$ (say), are all nourished by a single (other) compartment, say $x_0$ — they have no other significant intake. Recall that the original flow matrix was not stochastic. This leads to ambiguity in producing a stochastic matrix (alluded to earlier). The choice we make here is to have the diagonal of $R$ be zero. For $R_{x_0 x_i}$, $i = 1, 2, 3$, this means that each of these entries is unity. Equation (1) then becomes $\lambda_k A_k(x_0) = A_k(x_i)$, $i = 1, 2, 3$. If we now further assume that the $\lambda$s are not too different from one another (which seems to happen for the larger eigenvalues of the matrix under consideration), it follows that all $A_k(x_i)$ have essentially the same value — which means that they are located in the same place in the OR. An example of this is shown in Fig. 9, where compartments 90 and 99 are quite close in both the 1-2-3 and the 2-3-4 ORs. Checking actual consumption values, one does not have precisely the situation just discussed; rather these taxa, Mackerels and Other Pelagics, have substantially the same diet, largely in compartment 59, but with parallel patterns in other compartments. In Appendix B, we deal with the theory of the more general situation.

In the Florida Bay graph some compartments are tightly gathered, some are not. The herpetofauna and the avifauna (respectively) form tight clusters, while fishes and microfauna are all over the place. This remains true for other large
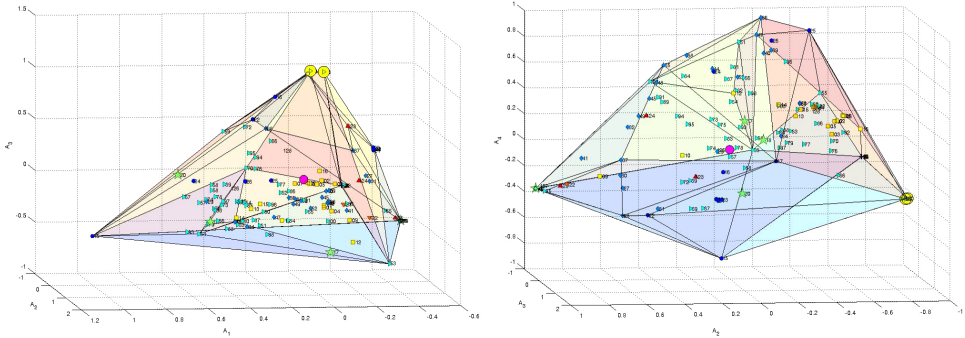
Fig. 9.    (Color online) OR for the Florida Bay system using eigenvectors [1–3] (left) and [2–4] (right). The yellow circles indicate the location of compartments 90 and 99, both of which have substantially the same diet.

eigenvalue ORs. Without greater ecological knowledge we can only speculate as to the significance of this sorting. Our guess is that the clustered creatures are top predators and within their groups are not all that different from one another in terms of diet. Fish (and certainly microfauna) can be both high and low on the food chain, so that it may be that a finer classification is in order. (We notice that there is some clustering in subclasses of fishes and macroinvertebrates.)

As remarked earlier, not all the observations made in the last paragraph can be gleaned from the figure provided. Rather, using MATLAB® software, the plotted figure was rotated, the marker sizes varied, the image magnified selectively, and other tricks of viewing were employed. We emphasize that the researcher using the OR will have all these tools available in the course of carrying out a similar analysis using any modern computational software.

We have also explored what one gets by looking at the OR for the transpose of the matrix $T$, given above. In this case all the primary producers are lumped together on one extremum of the convex hull for the lower eigenvalues. On the other hand, the microfauna appear to be on the outside. Interesting sorting of other creatures takes place, for example, herbivorous ducks are displaced somewhat from avifauna, but instead are quite close to herbivorous amphipods.

In the following, we summarize a number of observations we have made from the OR of the Florida Bay. At this stage we do not know if these are significant or not, and entries on the list can appear for diametrically opposed reasons: the OR is confirming some notion we have about the network or the OR is surprising us with something that seems *not* to make sense — and which we hope might be of interest to the expert for that very reason.

- Big herons and egrets (105) and Small herons and egrets (106) are close to one another but not as close as some of the other avifauna. Perhaps these compartments are overly general and some details have been lost and this is picked up by the OR?

- Odd couples: Manatees (122) and Herbivorous ducks (109) are close together. Cormorant (104) and Predatory ducks (111) are grouped very closely with Small shore birds (114) nearby.
- Loggerhead (118), Green (119), and Hawksbill (120) turtles are all very close together, with Crocodiles (117) nearby but clearly separated. This relationship remains regardless of which slow eigenvectors are plotted. Has the OR picked up fundamental similarities and differences between herpetofauna? See Appendix B for interpretive tools.
- Oithona nana (19) and Paracalanus (20) are very close while Other copepoda (21) are nearby but separated. The Grey snapper (80) is also (curiously) nearby. Grey snappers tend to feed on larger crustaceans but some copepoda have been known to parasitize grey snappers. Is this information present in the trophic network and the OR is showing it, or has the OR *predicted* such a possible relationship?
- The rough overall shape consists of a tilted triangular plane of points dominated by primary producers on one side; macroinvertebrates on another; and fishes, avifauna, and herpetofauna on the third. The inner region contains mostly fishes, but some microfauna and primary producers also appear there.
- We comment further on the fact that the Detritus sits at the extrema of the convex hull. The eigenvalue spectrum of the matrix does not have the near-degeneracy associated with phase transitions, so this does not mean that these are dynamically mutually inaccessible. It does suggest though some degree of specialization among detritus feeders.

### 3.2. *Yeast proteins*

We next present the OR of the yeast protein interaction network [19]. We limited the network (provided in the supplementary materials of [19]) to interactions of highest confidence, yielding a graph of 573 proteins and 2097 interactions. The matrix resulting from the associated graph and its pseudo-dynamics is reducible, and only its restriction to its largest component is studied. The proteins are either grouped into functional categories or are listed as uncharacterized.

As shown in Fig. 10, the OR of the yeast network has a structure consisting of multiple filaments or threads (see Appendix C) emanating from a densely clustered central region near the origin. Many of these threads correspond to the functional groups to which the proteins belong. This, coupled with the presence of uncharacterized proteins, may allow for predictions of protein functionality based on the protein's location in the OR and its relative proximity to other proteins.

The "threads" are reminiscent of structures seen in the lexicon network of Chavalarias [20]. In Fig. 11 we show both networks, rotated so that their similarity can be seen. In both cases lines peel away from the main body. (This was our motivation for the study in Appendix C.) The resemblance also leads to the question of whether the features seen in Chavalarias' lexicon study are reflected in
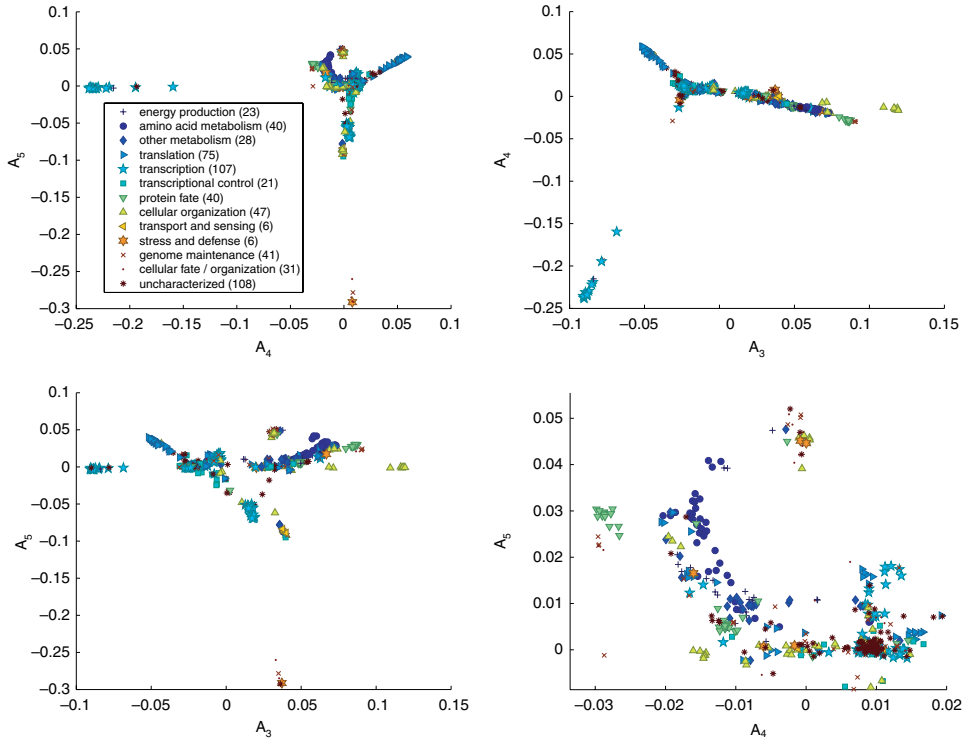
Fig. 10.    (Color online) Several views of the OR for the yeast protein interaction network discussed in Sec. 3.2. The first three figures show combinations of $A_3$ through $A_5$, while the last shows a magnification of the area near the origin in the $A_4$ versus $A_5$ plot. Many of the visible threads correspond strongly to functional categories, while the central region also shows some clustering based on protein function. Perhaps the distance from the origin (in $\mathbb{R}^n$) motivates a centrality measure, ranking which proteins are "more important" than others?

protein relationships. The lines in his work reflected specializations. (There is also a kind of inverse matrix in his work that approximately inverts relationships.) We also suspect that in higher dimension many of these lines are orthogonal (approximately), as for the star diagram in Ref. 4.

For the lexicon, the amateur can offer opinions: these are also words in ordinary English and one can easily guess relationships. For the proteins it will take an expert to make best use of this display.

### 3.3.  *Gene expression in the tissues of AIDS patients*

In the following example, the OR picks out two members of a population as being different. We do not know exactly what differences the OR is sensitive to, but we do know that two members of this population *are* different, and we believe that the OR has selected those individuals.
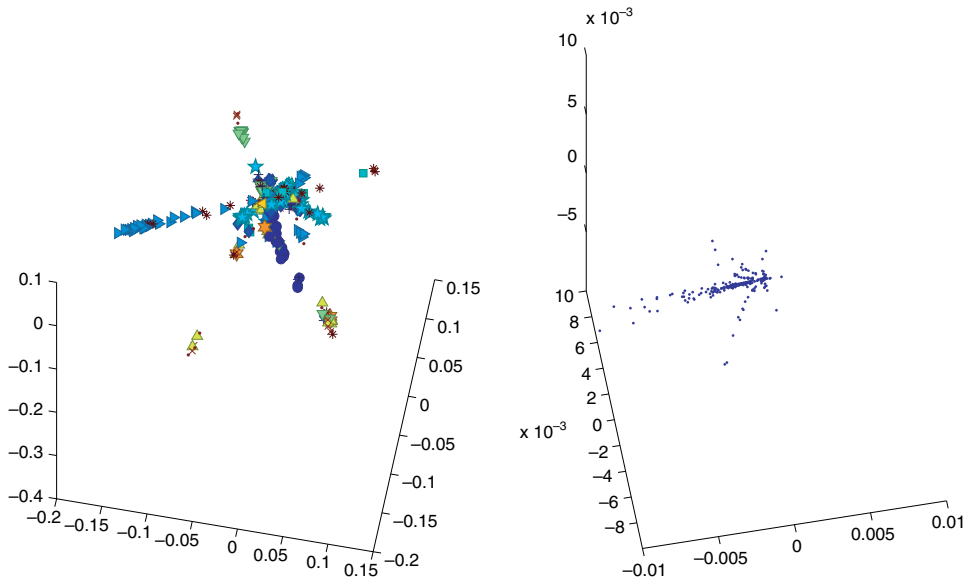
Fig. 11.  Comparison of yeast OR with that of Chavalarias's lexicon.

The population consists of 10 patients who have undergone an experimental AIDS treatment. The duration of the treatment was 32 weeks and two tissue samples were taken from each patient on three occasions: at the beginning, after 6 weeks, and at the end (32 weeks), for a total of 60 samples. These samples were studied[e] to determine which (of the many thousands of) genes in the tissues were expressed. Based on this, correlations as well as a distance function were defined between the samples.

From these data, we constructed a matrix, not of transition probabilities, but of the inverses of the distances. We do not have a systematic justification of why this should tell us anything about the trial. Nevertheless, as we now show, it revealed a grouping that would have been otherwise unnoticed. The precise construction is as follows: Let $D(i, j)$ be the distance function, with each "$i$" and "$j$" a number from 1 to 60. Person $k$, $k = 1, \ldots, 10$, gives rise to 6 samples, 2 at each testing interval. Thus, for example, the end-of-treatment tissues from person #3 are $k = 43$ and 53. We now let $\widetilde{R}(i, j) = 1/D(i, j)$, and finally arrive at $R$ by dividing $\widetilde{R}$ by its column sums. The diagonal is defined to be zero.

In Fig. 12 is the resulting plot. All 60 points are shown, with blue circles indicating (the 20) samples associated with the first measurement, the red crosses with the 6-week measurements, and the black stars the final 20 measurements. This OR is based on the first three non-trivial eigenvectors. It is clear that while the first

---

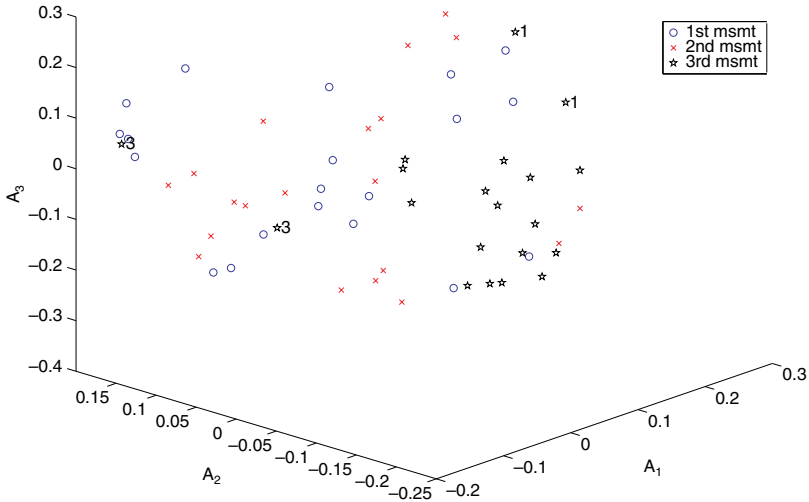[e]The data have been kindly provided by Arndt Benecke.

Fig. 12.   OR for eigenvectors $(1, 2, 3)$ for the AIDS study. Symbols represent the first ($\circ$), second ($\times$), and third ($\star$) set of measurements, respectively. For 2 pairs of end-of-treatment points we have indicated the code number of the associated individuals.

two sets are spread throughout the region, the final positions, the black stars, are far more concentrated in one region of the three-dimensional OR. Only four points stray from the cluster. It was easy to determine with which patients these points are associated and it turns out that they correspond to only two individuals, patients #1 and #3. In other words, while 8 of the patients responded to the treatment by arriving at a fairly uniform state of gene expression, for the two outliers gene expression did not move in the same direction.

Unfortunately, because this is an ongoing (at the time of writing) double-blind experiment, we cannot immediately say whether we have successfully flagged medically significant information. It is know that one of the ten patients withdrew from the study but continued to give tissue samples. It is also known that our group of ten was part of a larger population of 150 of whom three died. So there can very well have been a true phenomenon to diagnose, but we do not yet know whether the OR can serve as a tool for this purpose.

## 4. Some of the Underlying Principles

Why does this work? In dynamic terms (thinking of the Markov process), things that are placed together in the OR are able to reach each other in relatively short times. This needs to be qualified, taking into account details of eigenvalue structure as well as currents[f] for directed graphs. For example, for the no-current case we

---

[f]A current represents flow even in the stationary state. If $p_0(x)$ is the stationary state and $R_{xy}$ the matrix of transition probabilities, the current is defined as $J_{xy} \equiv R_{xy}p_0(y) - R_{yx}p_0(x)$.

have the following inequality.[g] Let $p_x(u, t)$ be the probability distribution at time $t$ of a system whose time-0 position was $x \in X$. Thus $p_x(u, t) = R_{ux}^t$. Define

$$D(x, y; t) \equiv \sum_u \left| \frac{p_x(u, t) - p_y(u, t)}{\sqrt{p_0(u)}} \right|, \tag{2}$$

with $p_0$ the stationary state. In Ref. 4 it is shown that

$$D(x, y; t) \geq \sqrt{\sum_\alpha |\lambda_\alpha|^t \, |A_\alpha(x) - A_\alpha(y)|^2}, \tag{3}$$

with $\lambda_\alpha$ the $\alpha$th eigenvalue (eigenvalues are labeled in order of decreasing magnitude, starting from $\lambda_0 = 1$). The sum on the right can be truncated at the $m$th eigenvalue, preserving the direction of the inequality. Since the magnitudes of the eigenvalues decrease monotonically with index we obtain

$$D(x, y; t)/|\lambda_m|^t \geq \sqrt{\sum_{\alpha=1}^m |A_\alpha(x) - A_\alpha(y)|^2}. \tag{4}$$

The quantity on the right is the distance in the observable representation. Thus, two points $x$ and $y$ that are adjacent dynamically — in the sense that the Markov chain soon nearly-forgets which point it came from — will be spatially adjacent in the OR.

For the many other properties that can be established, we again refer the reader to our earlier articles.

To round out the present section, we present new results on the way in which lines and other lower dimensional subspaces can occur in the OR. Define a thread as a collection of points in $X$ that communicate with the rest of $X$ through a single point of the thread. Calling that point, $x_0$, and calling the other points of the thread $x_1, x_2, \ldots, x_p$, we require that $R_{yx_k} = 0$ for $y$ not in the thread and $k = 1, \ldots, p$ (flow *into* the thread is allowed). Then, subject to certain limitations on the spectrum of $R$ restricted to the thread, the thread forms a straight line in the OR. One can also generalize this to higher dimension: *n-skeins* are defined to be subsets of $X$, like threads, except that $n$ points can take you to the rest of $X$ (so a thread is a 1-skein; we will also refer to 2-skeins as threads). In that case, and subject to similar assumptions on the spectrum, the skein forms an $n$-dimensional subset of whatever dimension OR is under consideration. The proof of these assertions is in Appendix C.

---

[g]When there are currents present the inquality developed in Eqs. (3) and (4) is usually obeyed, although we have not found a general way to characterize exceptions. For this inequality one uses the normalization $\sum p_0(x)|A_k(x)|^2 = 1$.

## 5. Discussion

Bear in mind that the theorems invoked here are generally speaking *sufficient* but not necessary. Exceptions do exist, as in our demonstration [2] that phase transitions (manifested as clustering at the extrema in the OR) imply eigenvalue degeneracy, and vice versa. However, in general, we do not have much information on the inverse problem: how to go uniquely from a pattern in the OR to properties of the matrix $R$.

Of the three biological examples that we considered we believe the most striking is the grouping of patients in the AIDS observable representation, very likely ferreting out a genetic precursor with predictive value. Is this because this problem is particularly susceptible to the OR? We do not think so. Rather, when investigating this system we had at our elbow the provider of the data (A. Benecke) whose questions and input spurred us to try one or another variation of the OR. We believe that in other fields as well an interested specialist would help realize the potential of this method.

## Appendix A.  Barycentric Coordinates

We give a two-dimensional example. Let the three 2-vectors $\boldsymbol{E}_k$, $k = 1, 2, 3$, define a triangle in the plane and let $\boldsymbol{P}$ be a point within that triangle (expressed as a 2-vector). Then the vector equation

$$\boldsymbol{P} = \sum_{k=1,2,3} \mu_k \boldsymbol{E}_k \tag{A.1}$$

uniquely defines the numbers $(\mu_1, \mu_2, \mu_3)$.[h] They are the barycentric coordinates of $\boldsymbol{P}$. When $\boldsymbol{P}$ lies in the interior (or on the boundary) of the triangle these numbers are non-negative and sum to one.

---

[h]To see this you can take the dot product of Eq. (A.1) with any 3 linearly independent vectors. The solvability of the resulting matrix equation depends on the 3 extrema not being colinear.

## Appendix B. OR Features when States have Similar Input or Output

As usual we have a stochastic matrix, $R_{xy}$ on a space $X$, with $x, y \in X$. We now assume $R_{xx} = 0$, a condition we can impose in associating a "transition matrix" with a graph. The left eigenvector/eigenvalue satisfies

$$\lambda_k A_k(x) = \sum_y A_k(y) R_{yx}. \tag{B.1}$$

Because of the zero-diagonal condition, $A_k(x)$ does not appear in the foregoing sum.

Fix an OR by choosing indices $k_1, k_2, \ldots, k_p$, and denote the corresponding vector

$$\boldsymbol{A}(x) = \begin{pmatrix} A_{k_1}(x) \\ A_{k_2}(x) \\ \vdots \\ A_{k_p}(x) \end{pmatrix} \in \mathbb{R}^p \text{ or } \in \mathbb{C}^p. \tag{B.2}$$

Then one can rewrite Eq. (B.1) as

$$\boldsymbol{A}(x) = \sum_{y \neq x} \begin{pmatrix} \frac{A_{k_1}(y)}{\lambda_{k_1}} \\ \frac{A_{k_2}(y)}{\lambda_{k_2}} \\ \vdots \\ \frac{A_{k_p}(y)}{\lambda_{k_p}} \end{pmatrix} R_{yx} = \sum_{y \neq x} \boldsymbol{W}(y) R_{yx}, \tag{B.3}$$

with

$$\boldsymbol{W}(y) = \begin{pmatrix} \frac{A_{k_1}(y)}{\lambda_{k_1}} \\ \frac{A_{k_2}(y)}{\lambda_{k_2}} \\ \vdots \\ \frac{A_{k_p}(y)}{\lambda_{k_p}} \end{pmatrix} \in \mathbb{C}^p. \tag{B.4}$$

Recall that by virtue of our assumption on the diagonal of $R$, $\sum_{y \neq x} R_{yx} = 1$.

Equation (B.2) represents $\boldsymbol{A}(x)$ as sum of vectors, $\boldsymbol{W}$, over positive quantities that sum to 1. *Therefore the OR point for $x$, namely $\boldsymbol{A}(x)$, is in the convex hull of those $\boldsymbol{W}(y)$ such that $R_{yx} \neq 0$.*

This leads to two observations about OR structure:

(1) Consider a collection of $x \in X$ such that in a single timestep all of them go to the same collection of $y \in X$. The associated $\boldsymbol{A}(x)$'s form a subspace (in the sense of linear algebra) of $\mathbb{R}^p$ (or $\mathbb{C}^p$, as the case may be).

(2) If $x_1$ and $x_2$ are such that $R_{yx_1} \approx R_{yx_2}$ for all $y$, then $\boldsymbol{A}(x_1) \approx \boldsymbol{A}(x_2)$.

These results are relevant to our study of the graph of Florida Bay ecology, Sec. 3.1.

## Appendix C. Threads and Skeins

The points of $X$ can be thought of as the nodes of a graph; there is a directed edge between the nodes $y$ and $x$ iff $R_{yx} \neq 0$.

Define a thread in $X$ to be a subset, $\{x_0, x_1, \ldots, x_p\} \subset X$, with the following properties.

(1) $(x_0, x_1, \ldots, x_p)$ are connected to one another in the graph (there's a path of (directed) non-zero $R$ matrix elements from any one to any other).
(2) For $2 \leq \ell \leq p - 2$,
$R_{yx_\ell} = 0$ if $y \notin \{x_1, x_2, \ldots, x_{p-1}\}$.
Note that probability can flow *in* from outside the thread, but it cannot flow out.
(3) For $\ell = 1$ or $\ell = p - 1$,
$R_{yx_1} = 0$ if $y \notin \{x_0, x_2, \ldots, x_{p-1}\}$,
$R_{yx_{p-1}} = 0$ if $y \notin \{x_1, x_2, \ldots, x_p\}$.

This can be generalized to an $n$-skein, with $n$ elements of the set in contact with the rest of $X$. A thread is a 1- or 2-skein. Our definition above is for a 2-skein.

Condition (2) means that the points $x_2, \ldots, x_{p-2}$ talk only to $\{x_1, x_2, \ldots, x_{p-1}\}$. Condition (3) means that $x_1$ talks to $\{x_1, x_2, \ldots, x_{p-1}\}$, and also to $x_0$ (similarly for $x_{p-1}$). Moreover, $x_0$ and $x_p$ can talk to any state in the graph.

These conditions imply that when the random walk on $X$ associated with $R$ enters the thread (which it can do from anywhere), it performs a random walk within the thread and can only exit via one of the points, $x_0$ or $x_p$.

Figure 13 suggests nearest-neighbor connectivity, although that is not required by our definition.
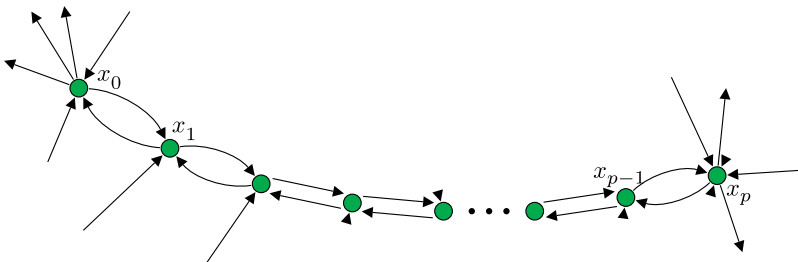


Fig. 13.　A 2-skein.

We prove the following property of the observable representation associated with $R$:

Consider the observable representation (OR) for a collection of eigenvectors $\{k_1, \ldots, k_n\}$,

$$\boldsymbol{A}(x) = (A_{k_1}(x), \ldots, A_{k_n}(x)) \in \mathbb{R}^n, \tag{C.1}$$

with eigenvalues $\lambda_{k_j} = \Lambda + \mathrm{O}(\epsilon)$ for $j = 1, \ldots, n$, for some $\Lambda$. Then up to order $\epsilon$, $\boldsymbol{A}$ maps a thread onto a plane, *and under some conditions, onto a quasi-one-dimensional curve.*

**Proof.** Let $k$ be in the set $\{k_1, \ldots, k_n\}$. For a left eigenvector $A_k$ of $R$, with eigenvalue $\lambda_k$, we write its defining equation at the points of the thread, bearing in mind the conditions above.

$$\lambda_k A_k(x_\ell) = \sum_{j=1}^{p-1} A_k(x_j) R_{x_j x_\ell}, \quad 2 \le \ell \le p - 2 \tag{C.2}$$

$$\lambda_k A_k(x_1) = \sum_{j=1}^{p-1} A_k(x_j) R_{x_j x_1} + A_k(x_0) R_{x_0 x_1}, \tag{C.3}$$

$$\lambda_k A_k(x_{p-1}) = \sum_{j=1}^{p-1} A_k(x_j) R_{x_j x_{p-1}} + A_k(x_p) R_{x_p x_{p-1}}. \tag{C.4}$$

Define

$$M_{j\ell} \equiv R_{x_j x_\ell}, \quad 1 \le j, \ell \le p - 1, \tag{C.5}$$

$$A_k(j) \equiv A_k(x_j), \quad 1 \le j \le p - 1. \tag{C.6}$$

Equations (C.2)–(C.4) can be rewritten as a matrix equation for row vectors:

$$A_k(\lambda_k - M) = (A_k(x_0) R_{x_0 x_1}, 0, \ldots, 0, A_k(x_p) R_{x_p x_{p-1}}). \tag{C.7}$$

Solving,

$$A_k = (A_k(x_0) R_{x_0 x_1}, 0, \ldots, 0, A_k(x_p) R_{x_p x_{p-1}})(\lambda_k - M)^{-1}. \tag{C.8}$$

Bearing in mind that the right-hand side of Eq. (C.7) has only 2 non-zero components, this can be explicitly written as

$$A_k(x_j) = A_k(x_0) R_{x_0 x_1}((\lambda_k - M)^{-1})_{1j} + A_k(x_p) R_{x_p x_{p-1}}((\lambda_k - M)^{-1})_{p-1,j}. \tag{C.9}$$

Now consider the OR for the given collection $\{k_1, \ldots, k_n\}$ labeling eigenvectors and eigenvalues:

$$\boldsymbol{A}(x) = (A_{k_1}(x), \ldots, A_{k_n}(x)) \in \mathbb{R}^n. \tag{C.10}$$

As stated, we assume that the eigenvalues $\{\lambda_k\}$ are close to one another, i.e., there is a $\Lambda$ such that $|\Lambda - \lambda_{k_j}| < \epsilon, \forall j = 1, \ldots, n$, for small $\epsilon$. Then by Eq. (C.9)

$$\boldsymbol{A}(x_j) = \boldsymbol{A}(x_0) a_j + \boldsymbol{A}(x_p) b_j + \mathrm{O}(\epsilon), \tag{C.11}$$

since $(\lambda_k - M)^{-1}$ is nearly independent of $k$.

Equation (C.11) implies that the thread lies in a two-dimensional subspace of the OR. With conditions on nearest-neighbor-only connections within the thread we expect that this will further imply that it actually lies on a line, as for our experience with Brownian motion, but we have not yet determined those conditions precisely.

Clearly, if there is only one point at which the thread is connected to the rest of $X$ (so the thread is a 1-skein) the OR subset for the thread lies on a line. In general, a $k$-skein ($k$ points talking to the rest of $X$) will lie in a $k$-dimensional subset of the OR (as follows from the number of non-zero contributions on the right-hand side of the equation for $\boldsymbol{A}$).

We remark that the spectral assumption on "$M$" is not trivial and when there is overlap with the eigenvalues of the $A$'s of the OR our result breaks down. This is because the inverse $(M - \lambda)^{-1}$ can be sensitive to small differences in the eigenvalues.

# References

[1] Gaveau, B. and Schulman, L. S., Master equation based formulation of non-equilibrium statistical mechanics, *J. Math. Phys.* **37** (1996) 3897–3932.

[2] Gaveau, B. and Schulman, L. S., Theory of non-equilibrium first order phase transitions for stochastic dynamics, *J. Math. Phys.* **39** (1998) 1517–1533.

[3] Gaveau, B. and Schulman, L. S., Multiple phases in stochastic dynamics: Geometry and probabilities, *Phys. Rev. E* **73** (2006) 036124.

[4] Gaveau, B., Schulman, L. S. and Schulman, L. J., Imaging geometry through dynamics: The observable representation, *J. Phys. A* **39** (2006) 10307–10321.

[5] Schulman, L. S. and Gaveau, B., Coarse grains: The emergence of space and order, *Found. Phys.* **31** (2001) 713–731.

[6] Von Luxburg, U., A tutorial on spectral clustering, *Stat. Comput.* **17** (2007) 395–416.

[7] Shi, J. and Malik, J., Normalized Cuts and Image Segmentation, *IEEE Trans. Pattern Anal. Machine Intell.* **22** (2000) 888–905.

[8] Zachary, W. W., An information flow model for conflict and fission in small groups, *J. Anthropol. Res.* **33** (1977) 452–473.

[9] Sherrington, D. and Kirkpatrick, S., Solvable model of a spin-glass, *Phys. Rev. Lett.* **35** (1975) 1792–1796.

[10] Schulman, L. S., Mean field spin glass in the observable representation, *Phys. Rev. Lett.* **98** (2007) 257202.

[11] Krause, A. E., Frank, K. A., Mason, D. M., Ulanowicz, R. E. and Taylor, W. W., Compartments revealed in food-web structure, *Nature* **426** (2003) 282–285.

[12] Girvan, M. and Newman, M. E. J., Community structure in social and biological networks, *Proc. Natl. Acad. Sci.* **99** (2002) 7821–7826.

[13] Ellson, J., Gansner, E., Koutsofios, E., North, S. and Woodhull, G., Graphviz and dynagraph — Static and dynamic graph drawing tools, in *Graph Drawing Software*, eds. Junger, M. and Mutzel, P. (eds.) (Springer-Verlag, 2004), pp. 127–148.

[14] Gaveau, B. and Schulman, L. S., Dynamical distance: coarse grains, pattern recognition, and network analysis, *Bull. Sci. Math.* **129** (2005) 631–642.

[15] Baird, D. and Ulanowicz, R., The seasonal dynamics of the chesapeake bay ecosystem, *Ecol. Monogr.* **59** (1989).

[16] Ulanowicz, R., Bondavalli, C. and Egnotovich, M., *Tech. Rep. Ref. No.* [UMCES] CBL 98–123, Chesapeake Biological Laboratory, Solomons, MD 20688-0038, USA (1998).

[17] Ulanowicz, R., Bondavalli, C. and Egnotovich, M., *Tech. Rep. Ref. No.* [UMCES] CBL 00-0176, Chesapeake Biological Laboratory, Solomons, MD 20688-0038, USA (1997).

[18] Kahn, P., From genome to proteome: Looking at a cell's proteins, *Science* **270** (1995) 369–370.

[19] von Mering, C., Krause, R., Snel, B., Cornell, M., Oliver, S. G., Fields, S. and Bork, P., Comparative assessment of large-scale data sets of protein-protein interactions, *Nature* **417** (2002) 399–403, http://dx.doi.org/10.1038/nature750.

[20] Private communication, David Chavalarias, CREA, Paris, see http://chavalarias. free.fr.